

Quantifying Uncertainty in Flow Functions Derived from SCAL Data

USS Relative Permeability and Capillary Pressure

S. SUBBEY^{1,*}, H. MONFARED^{2,3}, M. CHRISTIE³ and
M. SAMBRIDGE⁴

¹*Institute of Marine Research, PB 1870 Nordnes, N-5817 Bergen, Norway*

²*Heriot-Watt Institute of Petroleum Engineering, Edinburgh EH14 4AS, UK*

³*National Iranian Oil Company, Hafez Crossing, Taleghani Avenue, Tehran, Iran*

⁴*Research School of Earth Sciences, Institute of Advanced Studies, Australian National University, Canberra ACT 0200, Australia*

(Received: 1 June 2004; accepted in final form: 16 December 2005)

Abstract. Unsteady-state (USS) core flood experiments provide data for deriving two-phase relative permeability and capillary pressure functions. The experimental data is uncertain due to measurement errors, and the accuracy of the derived flow functions is limited by both data and modeling errors.

History matching provides a reasonable means of deriving in-phase flow functions from uncertain unsteady-state experimental data. This approach is preferred to other analytical procedures, which involve data smoothing and differentiation. Data smoothing leads to loss of information while data differentiation is a mathematically unstable procedure, which could be error magnifying. The problem is non-linear, inverse and ill posed. Hence the history-matching procedure gives a non-unique solution.

This paper presents a procedure for quantifying the uncertainty in two-phase flow functions, using unsteady-state experimental data. We validate the methodology using synthetic data.

We investigate the impact of uncertain flow functions on a homogeneous reservoir model using the Buckley–Leverett theory. Using a synthetic, heterogeneous reservoir model, we estimate the uncertainty in oil recovery efficiency due to uncertainty in the flow functions.

Key words: unsteady-state, relative permeability, capillary pressure, uncertainty, Buckley–Leverett, heterogeneous reservoir, oil recovery potential.

AMS Classifications: Primary 93A30; Secondary 74G75.

Nomenclature

c	Spline coefficients
C	Covariance matrix
f	Fractional flow

*Author for correspondence: e-mail: samuels@imr.no

J	Performance index
K_{ro}/K_{rw}	Relative permeability of oil/water
L	Length, distance
m	model
n_m	Model ensemble size
n_r/n_s	Number of models generated/resampled at each iteration step
$n_o, n_w, n_p,$	Empirical parameters
N_j^m	Spline basis function j of order m
$N_o N_w$	Cumulative volumes of oil and water, respectively
\mathcal{O}	Data
p	Probability
P	Pressure data
r_j	Relative probability of model j
S	Saturation
t	Time
u	Filtration velocity
x	variable

Greek

α, β	Empirical parameters
Δ	Difference
Δ_j	j-norm
δ_{ik}	Kronecker-delta function
η	frequency
μ	Viscosity
ϕ	Porosity
ρ	Density
σ	Standard deviation
τ	Autocorrelation time

Subscript/Superscript

c	Capillary
d	Data
iw	Irreducible water
nw	Non-wetting
o	Oil
or	Residual oil
s	Simulated
T	Total
w	Water
wc	Connate water
wf	Water shock front

1. Introduction

Relative permeability and capillary pressure data are imperative for the simulation of multiphase flow in porous media. In petroleum engineering this data is obtained from laboratory displacement experiments using core samples of the porous media.

The laboratory experiments for measuring relative permeability can be categorized into two distinct methods namely, steady state (SS) and unsteady-state (USS) approaches. A comprehensive summary of these methods is provided in Honarpour *et al.* (1986). This paper will be concerned with the unsteady-state method.

Initially, a core of length L , at an irreducible wetting phase (usually water) saturation S_{wc} , is fully saturated with a non-wetting phase (usually oil), i.e., the non-wetting phase saturation $S_{nw} = 1 - S_{wc}$. The unsteady-state (USS) approach involves injecting a single phase, (i.e., the wetting fluid) through one end of the core ($x = 0$). The injection occurs either at constant filtration velocity or constant difference pressure across the core. The escaping fluids are collected at the other end ($x = L$). The technique provides time series data in the form of cumulative volumes of each fluid and the pressure drop across the core. The attraction with the USS method lies in the fact that the experimental procedure is much quicker and less expensive than the steady state approach.

The drawback with the USS method, however, is that the flow functions are uncertain because they must be indirectly inferred from analysis of the experimental data. In interpreting USS experimental data, the equations are usually solved by methods of Buckley–Leverett (Buckley and Leverett, 1942; Welge, 1952) and Johnson, Bossler and Naumann (JBN). These methods are sometimes inadequate for defining relative permeability and capillary pressure functions for heterogeneous reservoir systems or for water displacing a very light oil in a homogeneous sandstone (Archer and Wong, 1973). The accuracy of the analysis is also affected by a combination of errors arising from the experiment (data errors) and the mathematical modeling of the experimental procedure (modeling errors).

In petroleum engineering, the standard approach to reducing uncertainty in modeling is by history matching. The literature shows that this approach has been applied to unsteady-state data in order to derive relative permeability functions and gradient type optimization algorithms have been used. The algorithms provide a single set of in-phase flow functions but give no guarantee that the derived functions represent optimal solutions.

This paper presents a procedure for deriving two-phase (oil/water) relative permeability and capillary functions from USS experiments. It also addresses the issue of quantifying uncertainty in the derived functions. Our procedure involves expressing the sought flow functions in terms of adjustable parameters which are determined through history matching the laboratory data. We generate multiple models, which match the laboratory data using a stochastic algorithm. Using the ensemble of models generated, we quantify uncertainty in the relative permeability and capillary pressure

functions in a Bayesian framework. This paper presents results on a synthetic data set. A future paper will look at an application to field data.

The paper is organized in the following way. Section 2 discusses the basic theory behind the experimental procedure, including equations of flow, initial and boundary conditions. Section 2.2 specifically discusses approaches for deriving flow functions from USS experiments. Sections 3 discusses the principal sources of uncertainty in deriving in-phase flow functions from USS data. Section 4 presents our proposed methodology, including functional representation of the flow functions while Section 4.2 gives a brief description of the sampling algorithm. This section also discusses the performance index definition and a procedure for resampling from the posterior distribution. Our validation procedure is presented in Section 5. This section describes the parameterization equations for the sought relative permeability and capillary pressure functions. Section 6 describes the models used in testing for the impact of the relative permeability and capillary pressure uncertainty on reservoir simulation and performance prediction. Our results are presented and discussed in Section 7. Finally, Section 8 gives a summary of our main results and conclusions.

2. Theory

This section gives a basic description of the theory for two-phase flow in the porous medium during a USS experiment and methodologies for deriving the flow functions from experimental data. For detailed literature about the theory, see, e.g., Willhite (1986).

We consider a core of length L initially containing water at irreducible saturation, S_{wc} , and oil at saturation $1 - S_{wc}$.

2.1. FLOW EQUATIONS AND MATHEMATICAL MODEL

We assume that the phases are incompressible, and that the experiment is carried out under isothermal conditions (i.e., the porosity ϕ , densities ρ_i and viscosity μ_i , are constants). The volumetric continuity equations describing the one-dimensional, two-phase flow are given by (1) and (2).

The flow velocity u_i in (1) is derived using the extended Darcy law (see Willhite, 1986). For a horizontal core of length L and origin at the inlet ($x = 0$), the initial and boundary conditions are derived from the experimental setup. Thus the initial conditions are those of uniform distribution of saturation and atmospheric pressure, while the boundary conditions consist of constant injection pressure P_{inj} and maximum attainable

water saturation of the core at the inlet, and outlet pressure P_L at the outlet. In (1) and (2), the index i designates oil (o) and water (w).

$$\partial_x u_i + \phi \partial_t S_i = 0, \tag{1}$$

$$\partial_x \sum_i u_i = 0, \quad \sum_i S_i = 1. \tag{2}$$

For a chosen water injection rate, $u_w(t)$, the classical experimental procedure provides data for the difference pressure across the core, $\Delta P = P_L - P_{inj}$, and the cumulative volumes of oil and water at the core end, respectively, N_o and N_w . The aim is to use the measured data to determine the relative permeability functions, $k_{ri}(S_w)$, and the capillary pressure, $P_c(S_w)$, of the porous medium.

2.2. THE METHODOLOGIES FOR DERIVING FLOW FUNCTIONS

The literature contains several methods for deriving flow equations using unsteady-state data and the mathematical model.

It is customary to introduce new parameters into the equations above, which simplify the mathematical analysis. One such parameter is the fractional flow f_i of phase i defined by

$$f_i(t) = u_i(t) / (u_o(t) + u_w(t)) = u_i(t) / u(t). \tag{3}$$

Using the derived parameters, it is possible to derive analytical expressions for the sought flow functions in terms of the laboratory data (see Collins, 1976; Marle, 1981). Some simplification, e.g., the JBN (Johnson *et al.*, 1959) model, is introduced into the system in order to obtain computational ease. The JBN equations are perhaps the most commonly used sets of equations for deriving relative permeability functions from USS experiments.

The JBN model is based on the Buckley–Leverett (Buckley and Leverett, 1942) equation but the classical method suffers from capillary end effects, i.e., capillary pressure discontinuity at the ends of the core. Experimentation using high flow rates (where viscous forces dominate capillary pressures) have been suggested to address the problem (Osoba *et al.*, 1951; Richardson *et al.*, 1952; Willhite, 1986). Neglecting capillary forces result in inadequate models for heterogeneous cores, high viscosity oils or for low flow rate experiments in which capillary pressure terms may be significant (Archer and Wong, 1973; Sigmund and McCaffery, 1979). High flow rates are also uncharacteristic of petroleum reservoirs. The method also requires data differentiation, which is mathematically unstable, and/or data smoothing, which may lead to loss of information.

Results in Tao and Watson (1984) present a mathematically stable JBN approach, which involves using B-spline data interpolation. A point-wise

Monte Carlo confidence interval, based on synthetic data perturbation, is established. The application of the uncertainty quantification procedure to real data may have limitations.

Semi-analytical methods have been put forward in Civan and Donaldson (1987, 1989), which account for capillary pressure effects. Integral and differential quadrature approximations were introduced to simplify the mathematical procedure. Uncertainty in the solution was not quantified.

Irrespective of the accuracy of the analytical or semi-analytical expressions, the methodologies fail to adequately account for how the errors in the experimental data and the uncertainties resulting from simplifying assumptions in the mathematical model, impact on the derived flow functions.

History matching provides a viable alternative, which can overcome the limitations of the analytical and semi-analytical approaches. Methods for deriving flow functions through history matching are well documented in the literature (see, e.g., Sigmund and McCaffery, 1979; Chavent *et al.*, 1980; Savioli and Bidner, 1982; Kerig and Watson, 1987; MacMillan, 1987; Richmond and Watson, 1990).

History matching involves a non-linear approach for the determination of parameters. It involves a numerical simulator of the unsteady state, one-dimensional, two-phase flow and a functional representation of relative permeability and capillary pressure functions in terms of adjustable parameters. By varying the parameters, several models could be generated. The quality of each generated model is judged on the basis of a performance index, which is expressed in terms of the difference between the observed laboratory data and the model prediction.

A reservoir simulator is a numerical approximation of the continuous conservation and partial differential equations describing the multiphase flow in porous media with discrete analogues. Simulators reported in the literature include those based on finite difference methods (Sigmund and McCaffery, 1979; Chaven *et al.*, 1980; Kerig and Watson, 1987; MacMillan, 1987; Richmond and Watson, 1990); or a finite element approach (Chavent *et al.*, 1980). One solves explicitly for the saturation values, while the pressure values are implicitly evaluated (see e.g., Gabbanelli *et al.*, 1982).

Different parameterizations of the flow equations have been reported, and include the use of splines (Kerig and Watson, 1987), and power functions (Sigmund and McCaffery, 1979; MacMillan, 1987; Grattoni and Bidner, 1990).

The measure of the performance index reported in the literature, has been least squares (Grattoni and Bidner, 1990) or a variant, e.g., weighted least squares (Kerig and Watson, 1987), and gradient type algorithms, e.g., Levenberg–Marquardt algorithm (Gill and Murray, 1981) are used. The results are a single set of flow functions of relative permeability and capillary pressure.

3. Uncertainty

Several authors (see e.g., Archer and Wong, 1973; Tao and Watson, 1984a, b) have indicated that there is a large degree of uncertainty in the flow functions derived from unsteady-state data. The uncertainty is due to both data and modeling errors.

A major source of model error is the simplifying assumptions in the mathematical model. An example is the assumption that the core is homogeneous. It is well established that reservoir rocks, even though appearing to be homogeneous on core scale, are usually heterogeneous. If derived flow functions are to be applied to field simulations, a more accurate approach would be to consider heterogeneous cores. The assumptions that the phases are incompressible, and that the experiment is carried out under isothermal conditions could be violated when dealing with heavy oils; (see Akin *et al.*, 1999).

In using a history matching procedure, the standard approach is to choose a functional representation of relative permeability and capillary pressure functions, expressed in terms of adjustable parameters. For the history matching procedure to be successful, it is imperative that the following two issues are addressed namely,

- the choice of functional representation of the flow functions,
- restricting the span of each model parameter on the real line, i.e., parameter ranges from which to sample.

The two issues are connected and readily extend to all cases of history matching involving the determination of flow functions, conditioned to observed data. In some cases the range could be restricted by a preliminary strategy; (see, e.g., Subbey *et al.*, 2002).

Perhaps the two most popular functional representations reported in the literature are those due to Corey (1954) and Chierici (1981). The former uses a power law functional representation while the latter uses an exponential function in representing the flow functions. Equations (4) and (5) represent the water relative permeability functional representations by Corey (1954) and Chierici (1981), respectively.

$$F(S, a) = [(S - S_{wc}) / (1 - S_{wc} - S_{or})]^a, \tag{4}$$

$$F(S, \alpha, \beta) = e^{-\alpha R^{-\beta}(S)}; R(S) = [S - S_{wc} / (1 - S_{or} - S)]. \tag{5}$$

The parameters (a for Corey, (α, β) for Chierici) do not carry any direct physical interpretation.

Rigid analytical functions, however, could be unable to capture relative permeability effects due to small-scale local heterogeneities in the cores. This could introduce uncertainties into the history matching process. We

illustrate with an example using (4) and (5). Taking (4) as the truth, it is possible to determine whether (5) is able to reproduce the truth by solving (6) for (α, β) over a defined saturation domain.

$$F(S, \alpha, \beta) \approx F(S, a). \tag{6}$$

We solved (6) using a stochastic algorithm (to be described), in the range $0 \leq \alpha, \beta \leq 10$, $a = 2$ and $0.2 \leq S \leq 0.8$. This gave an absolute minimum at $\alpha^{opt} = 1.355$ and $\beta^{opt} = 0.795$. Figure 1(a) shows the surface defined by the triplet $(\alpha, \beta, \Delta_2 F)$. We define $\Delta_j F$ as the norm- j of the difference between the Chierici and Corey functions, i.e.,

$$\Delta_j F = |F(S, \alpha, \beta) - F(S, a)|_j. \tag{7}$$

Our results show that $\Delta_j F$ is never zero. Hence if the truth is a Corey/Chierici curve, it is impossible, even in the absence of experimental error, to capture this truth. Figure 1(b) shows results of 50 slight perturbations in the values of α^{opt} and β^{opt} . The curves show perturbations of the Chierici function. Here, perturbation is defined by $\Delta_1 F$. The α and β values in Figure 1(b) apply to the curves to which the arrows point. These bounding curves demonstrate the sensitivity of the Chierici curves to slight perturbations in the parameters.

4. Proposed Methodology

The approach in this paper is to parameterize the relative permeability and capillary pressure functions using a flexible functional representation, which is capable of capturing local effects, e.g., of core heterogeneities.

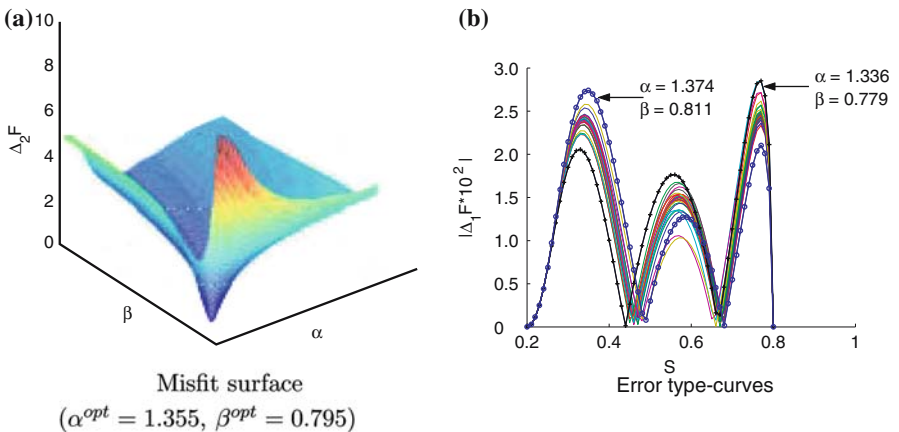


Figure 1. Misfit surface and sensitivity of derived function.

Using the experimental data, we determine the model parameters through a history matching procedure using a conventional, commercial, finite-difference simulator. Our approach is to generate an ensemble of models, which match the water flood data. Ultimately, we use the ensemble of models generated to quantify uncertainty in the derived flow functions in a Bayesian framework.

We use the Neighbourhood Approximation algorithm, which is a stochastic algorithm, in sampling for multiple models. The Neighbourhood Approximation (NA) algorithm has been described in earlier work (see e.g., Subbey *et al.*, 2002a,b).

4.1. PARAMETERIZATION

We parameterize the relative permeability and capillary pressure functions using normalized B-splines, which have support only on a limited part of the interval [0 1]. For detailed literature on splines, see Schumaker (1981).

We follow the same approach as in Watson *et al.*, (1998) and represent the flow function ($K_{ri}(S)$ and $Pc(S)$) by the general function $F(S)$ in (8), where n is the spline dimension and m is the spline order. The index i refers to oil (o), water (w) or capillary pressure (p).

$$F(S) = \sum_{j=1}^n c_{j,i} N_j^m(S) \tag{8}$$

Normalized B-spline representation of the flow functions offers a viable solution to the problem of range determination since the flow functions and the coefficients, $\{c_{j,o}, c_{j,w}, c_{j,p}\}$ take values within the same range as the basis functions, i.e., [0 1]. Further, one avoids the need to rescale the sampling space, which could be desirable in cases where the differences in the dimensions of the parameters are significantly high. Since the flow functions are monotone functions of saturation, we impose monotonicity constraints on the solution by an ordering of spline coefficients (see, e.g., Schumaker, 1981; Subbey, 2000).

We use the Neighbourhood Approximation Algorithm in sampling for the model parameters.

4.2. THE NEIGHBOURHOOD APPROXIMATION ALGORITHM

The Neighbourhood Approximation (NA) algorithm is a stochastic algorithm, which was originally developed by Sambridge (1998, 1999) for solving a non-linear inverse problem in seismology. The algorithm firstly identifies regions in the parameter space, which give good match to the observed or measured data. It then preferentially samples the parameter

space in a guided way, and generates new models in the good fit regions. It uses Voronoi cells to represent the parameter space.

The algorithm uses information obtained from previous runs to bias the sampling of model parameters to regions of parameter space where a good fit is likely. In this way it attempts to overcome one of the main concerns of stochastic sampling, i.e., poor convergence. A full description of the algorithm is given in Sambridge (1990).

Specifically, the NA algorithm generates multiple models iteratively in parameter space in the following way. First, an initial set of n_s models are randomly generated. In the second step, the n_r best models among the total number of model generated so far are determined. The n_r models are chosen on the basis of a performance index, i.e., the misfit function, which we discuss shortly. Finally, new n_s models are generated by uniform random walk in the Voronoi cells of each of the n_r chosen models. Thus at each iteration, n_r cells are resampled and in each Voronoi cell, n_s/n_r models are generated. The ratio n_s/n_r controls the performance of the algorithm.

For earlier applications of the algorithm in petroleum engineering (see Subbey *et al.*, 2002a, b, 2004).

4.3. DEFINING THE PERFORMANCE INDEX

Let $\mathcal{C} \in \mathcal{R}^n$ define the set of the n model parameters, i.e.,

$$\mathcal{C} = \{c_1, \dots, c_n\}. \quad (9)$$

We define $\Delta\bar{\mathcal{O}}$ as the difference between the measured/observed data, $\bar{\mathcal{O}}$, and that predicted by the model, $\mathcal{O}(m(\mathcal{C}))$, on basis of a sampled set of parameters. Thus $\Delta\bar{\mathcal{O}}$ is a non-linear function of \mathcal{C} , defined by (10).

$$\Delta\bar{\mathcal{O}} = \bar{\mathcal{O}} - \mathcal{O}(m(\mathcal{C})). \quad (10)$$

In the least square sense (Tarantola, 1987) the measure of misfit, J , is given by (11).

$$J = \sum_i \delta_{ij} \langle \Delta\bar{\mathcal{O}} | C^{-1} | \Delta\bar{\mathcal{O}} \rangle_i, \quad i = o, w, p. \quad (11)$$

By our definition, $j = i$ only if dataset i is included in the calculation. Thus δ_{ij} is identical to the Kronecker-delta symbol. For each dataset i , the total covariance matrix is defined by C . This matrix captures both the model and data errors. In modeling, several methods exist for defining the covariance matrix. The use of error models is an example (see Glimm *et al.*, 2001 a, b; O'Sullivan and Christie, 2004, submitted).

This paper presents results where the data covariance matrix structure, is defined by an exponential model, which takes into account the time correlation of the errors:

$$C^d(t_i, t_k) = \sigma_d^2 e^{-|t_i - t_k| \tau^{-1}}. \tag{12}$$

In (12) τ defines the lag i.e., the time interval over which the errors are assumed to be correlated, and σ_d is the variability expected in the data.

We have assigned different values to the parameters in (12) for water and oil volumes. We have assumed that the water volume is correlated over the whole time interval, while the oil data is correlated until breakthrough time. Further, estimates of σ_d are based on the standard deviation of the observed data. A further assumption is that the model errors are negligible compared to the data errors. For each model m_j generated, the degree of likelihood p , that the observed data $\bar{\mathcal{O}}$ is obtainable given the model is defined as

$$p(\bar{\mathcal{O}}|m_j) \sim e^{-0.5J}. \tag{13}$$

The refinement criterion for the NA sampling algorithm is based on the rank of the misfit. The misfit ξ is defined as $-\log$ of the likelihood. Thus

$$\xi_j = -\log p(\bar{\mathcal{O}}|m_j). \tag{14}$$

4.4. APPRAISING THE ENSEMBLE – SAMPLING FROM THE POSTERIOR

Bayesian theory provides the ultimate means of quantifying uncertainty in model performance. For a discussion on the benefit of a Bayesian approach over other traditional methods of uncertainty analysis, see, e.g., Sivia (1996) and Hensen *et al.* (1997).

In Bayesian analysis, prior belief about the uncertainty of each model before the experimental data is taken into account, is expressed through a prior probability density function $p(m)$. In the absence of any prior information, assigning equally likely probabilities to the models is a sound paradigm. With the observed laboratory data at hand, the prior is modified to yield a posterior probability function $p(m|\bar{\mathcal{O}})$ of the models given the laboratory data. Equation (15) gives an expression for the posterior probability.

$$p(m|\bar{\mathcal{O}}) = p(\bar{\mathcal{O}}|m)p(m) / \int p(m|\bar{\mathcal{O}})p(m)dm. \tag{15}$$

The likelihood probability $p(\bar{\mathcal{O}}|m)$ comes from a comparison of the laboratory data to the data obtained on the basis of the model. We

recall that the observed laboratory data is contaminated with errors. Hence comparison of observations with solutions derived from the model will have additional errors associated with uncertainties in the solution process.

One of the challenges in implementing (15) lies in the evaluating $\int p(m|\bar{O})p(m)dm$. The task of evaluating this (normalizing) constant is usually non-trivial, even for problems of very low dimension. Hence approximate methods for sampling from the posterior, which avoid explicitly evaluating this term, are attractive. Markov Chain Monte Carlo (MCMC) methods generate samples from the posterior distribution without calculating the normalizing term. MCMC methods require running chains of walks on the posterior distribution surface. New models are created in the process, and these models are either rejected or accepted based on a selected criterion.

To resample from the posterior distribution, the NA-Bayes algorithm uses a Gibbs sampler (Geman and Geman, 1984; Sambridge, 1999). The principle is to replace the true posterior probability density function with its neighborhood approximation, where specifically,

$$p(m) \approx p_{\text{NA}}(m). \quad (16)$$

Here $p_{\text{NA}}(m)$ is the NA approximation of the posterior probability distribution $p(m)$ for model m . This approximation is at the heart of the algorithm.

5. Validation

We validate our methodology using synthetic data. This testing phase of the methodology using synthetic data is important since the truth is known, and we can make quantitative assessments of the results. The next section describes the synthetic data model.

5.1. THE SYNTHETIC MODEL

Our model is partly taken from Grattoni and Bidner (1990). The relative permeability and capillary pressure curves are defined by

$$k_{\text{ro}}(S) = k_{\text{ro}}^* [(1 - S - S_{\text{or}})/(1 - S_{\text{wc}} - S_{\text{or}})]^{n_o}, \quad (17)$$

$$k_{\text{rw}}(S) = k_{\text{rw}}^* [(S - S_{\text{wc}})/(1 - S_{\text{wc}} - S_{\text{or}})]^{n_w}, \quad (18)$$

$$P_c(S) = P_c^* [(1 - S - S_{\text{or}})/(1 - S_{\text{wc}} - S_{\text{or}})]^{n_p}. \quad (19)$$

Equation (17)–(19), with $n_w = 2.5$, $n_o = 3.0$, $n_p = 5.0$, and information in Table I, constitute the true model description. We fed the model

Table I. Core and model parameters

A (cm ²)	11.041	μ_w (Pas)	0.99×10^{-3}
L (cm)	5.5	μ_o (Pas)	14.75×10^{-3}
ϕ	0.205	Pi_w (Pa)	1.80×10^5
k (μm^2)	35.0×10^{-3}	k_{ro}^*	0.865
S_{wc}	0.238	k_{rw}^*	0.300
S_{or}	0.228	P_c^* (Pa)	0.402×10^{-5}

information into a commercial, finite difference simulator and generated true cumulative oil and water production, as well as the difference pressure across the core, respectively, N_o^{tr} , N_w^{tr} and ΔP^{tr} . We generated 50 values of the true data in the saturation range $S_{wc} \leq S \leq 1 - S_{or}$, and added random noise to the true data in order to generate the experimental data $\bar{O} \equiv \{N_o^e, N_w^e, \Delta P^e\}$, according to (20) and (21). The random noise was generated, by drawing from a random normal distribution with zero mean and unit variance.

$$\Delta P^e(t_j) = \Delta P^{\text{tr}}(t_j) + \epsilon_j^{\Delta P}, \quad (20)$$

$$N_i^e(t_j) = N_i^{\text{tr}}(t_j) + \epsilon_{i,j}^N, \quad i = o, w; j = 1, \dots, 50 \quad (21)$$

We have investigated with different error levels in the experimental data. In the particular examples presented in this paper, we assume negligible errors in the pressure data. This is justified by the fact that modern methods for measuring pressure in the laboratory are extremely accurate. Hence any errors in the pressure data is usually several orders of magnitude lower than in the volume measurements.

6. Impact of Relative Permeability and Capillary Pressure Uncertainty

The aim is to investigate the impact of the uncertainties in relative permeability and capillary pressure on reservoir simulation and model prediction.

Our first example involves a homogeneous water flood model where capillary pressure effects are neglected. We investigate how the uncertainties impact on e.g., the recovery factor and prediction of water breakthrough time.

Our second model is a heterogeneous model. Both relative permeability and capillary functions are defined. Here, we investigate the effect of the uncertainties on the recovery efficiency of the reservoir. The next sections describe our models.

6.1. HOMOGENEOUS MODEL

We investigate the effect of the quantified relative permeability uncertainties on the performance of a homogeneous reservoir. We use the Buckley and Leverett (1942) theory of frontal advancement. Thus we neglect the effects of capillary pressure and investigate the sole impact of relative permeability uncertainty on front advancement, breakthrough time and recovery factor, for a homogeneous porous medium.

The Buckley–Leverett frontal advance theory involves equations, which allow for the estimation of, among others, the rate of frontal saturation movement, breakthrough time and recovery efficiency, during water flooding of a homogeneous porous medium. For example, the initial state could be an oil-saturated reservoir (at $S_w = S_{iw}$). If the reservoir is being flooded with water at a rate of Q_w , then the distance, X_f , traveled by the frontal saturation can be related to the volume of the water injected, N_w , and the gradient of the fractional flow at the front with respect to saturation by (22).

$$X_f = (Q_w / \phi A) \partial_{S_w} f_w |_{S_{wf}}, \quad (22)$$

where S_{wf} refers to the saturation of the displacement front, and the water breakthrough time, t_b , is given by (23).

$$t_b = (LA\phi Q_T^{-1}) / \partial_{S_w} f_w |_{S_{wf}}. \quad (23)$$

In (23), $Q_T = Q_w \cdot t_b$. After breakthrough, the average water saturation of the porous medium will increase with increasing water injection and climax at $(1 - S_{or})$. For detailed discussions on the Buckley–Leverett theory, see Archer and Wall (1991), Craig (1971) and Willhite (1986). Ensuring saturation (and velocity) continuity in the core requires the introduction of a saturation shock or step change at points where the fractional flow curve suggests a decreasing velocity with increasing distance.

It can be shown that (24) must be satisfied to ensure saturation and velocity continuity across the shock, where “+” and “−” denote parameters in front and behind the shock, respectively, which also shows that for $S_w^+ = S_{iw}$, $f_w^+ = 0$. In this paper, our approach involves interpolating the fractional flow data using spline functions. This approach eases the problem of data differentiation. We then determine S_{wf} by solving (24).

$$\Delta f / \Delta S = (f_w^- - f_w^+) / (S_w^- - S_w^+) = \partial_{S_w} f_w |_{S_{wf}}. \quad (24)$$

6.2. HETEROGENEOUS RESERVOIR SIMULATION MODEL

Given that petroleum reservoirs are seldom homogeneous, the aim here is to investigate whether the small-scale (core-scale) uncertainties in the flow

functions could have significant impact on important heterogeneous reservoir parameters. For this particular case, the truth corresponds to the reservoir model with the true (error-free) relative permeability and capillary pressure curves. The aim is to investigate to what degree the uncertainties in the flow functions affect, e.g., the oil recovery efficiency of the reservoir.

The original fine grid is a geostatistical model. It is represented in a three-dimensional domain $[(x, y), z] \in \mathcal{R}^2 \times \mathcal{R}$, being $[1200 \times 2200 \times 170]$ feet³, and discretized into $[60 \times 220 \times 85]$ cells. The model consists of two distinct geological formations. For a full description of the model as well as details of the fluid properties, see Floris *et al.*, (1999) and Christie and Blunt (2001).

We generated a coarser grid model consisting of $5 \times 11 \times 10$ grid cells, using single phase upscaling of the fine grid (Christie, 1996). There are four producers in the four corners of the model ($P1 - P4$) and a central injector ($I1$). All wells are vertical and penetrate up to the eighth layer of the vertical column.

In Christie and Blunt (2001), the rock curves consisted of a single pair of oil–water relative permeability curves with zero capillary pressure. We follow the same approach and represent the rock curves by a single set of oil–water relative permeability curves but include capillary pressure. The true heterogeneous model corresponds to running the coarse grid model with the true (error-free) set of flow functions. The ensemble of coarse grid solutions was obtained based on the ensemble of generated (sampled) flow functions.

A more rigorous approach will be to use flow functions generated by history-matching data generated by using heterogeneous cores, and including multiple flow regions. Indeed, there are several possible extensions of this methodology. However, this is beyond the scope of this paper.

7. Results and Discussions

We generated 1000 models by sampling a 13-parameter space; 4 parameters each for the oil and water relative permeability functions and 5 parameters for the capillary pressure function. These parameters are the spline coefficients. Unless otherwise stated, the units for capillary pressure curves will be in atmospheres.

Figure 2(a) shows a plot of the model misfit as a function of model index. The graph shows how the NA algorithm slowly adapts the sampling to low misfit regions of the parameter space. Figure 2(b)–(d) show the functions generated for the capillary pressure, water, and oil relative permeability functions, respectively.

The accuracy of the maximum likelihood model could also be observed in the way it predicts the in-phase flow functions in Figure 3(a) and (b).

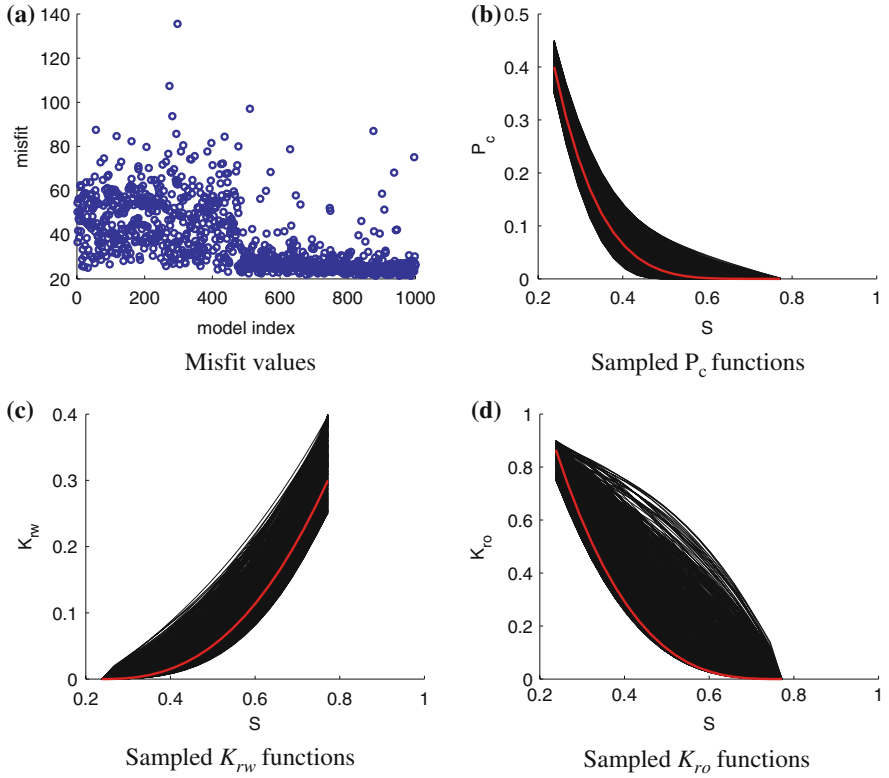


Figure 2. Sampling results.

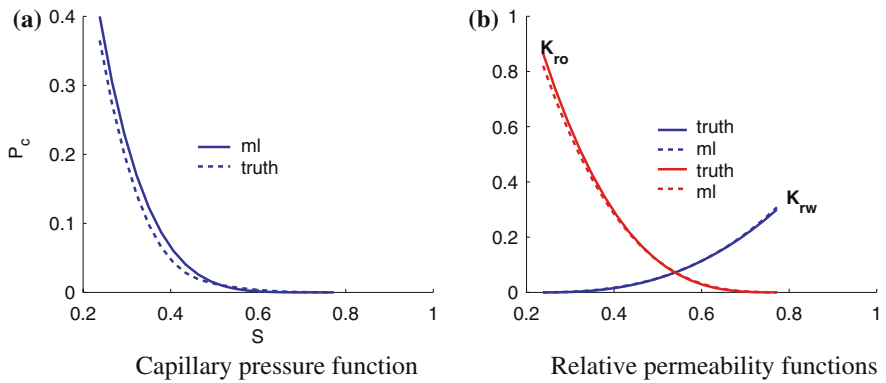


Figure 3. Maximum likelihood model performance.

We resampled from the posterior distribution by running a long MCMC chain (10^5) on the misfit surface and performing a Bayes update of the probabilities. The resampling process provides a good approximation to the whole posterior probability density functions for the desired functions and parameters. However, for the purpose of illustration, we adopt the following procedure. We monitored the frequency of visits to each Voronoi cell during the random walk. Thus we were able to calculate the relative probability r_j of each model m_j in an ensemble of size n_m , based on the frequency ψ_j , using

$$r_j = \psi_j / \sum_{k=1}^{n_m} \psi_k. \quad (25)$$

Assuming \mathcal{F} is our function of interest, we calculate the first and second moments of the sought function from

$$\langle \mathcal{F} \rangle_1 = \sum_k r_j \mathcal{F}_k, \quad (26)$$

$$\langle \mathcal{F} \rangle_2 = \sum_k r_j \mathcal{F}_k^2 - [\langle \mathcal{F} \rangle_1]^2. \quad (27)$$

Using these parameters, we calculated the 10th and 90th percentiles, P_{10} and P_{90} , respectively, for the parameters of interest.

It has been considered that there is uncertainty along the whole length of the functions. This is slightly different from convention where the end-points of the functions are determined experimentally and assumed known. Figure 4(a) and (b) show the uncertainty envelopes for capillary pressure and relative permeability functions, respectively. The truth, mean, and maximum likelihood (ml) functions are also plotted in the respective graphs. The uncertainty envelopes predicted by the algorithm rightly encapsulate the true functions.

To quantify the uncertainty in a homogeneous reservoir model performance, due to the uncertainty in the relative permeability curves, we investigated using different combinations of the functions in Figure 4. We used analytical expressions from the Buckley–Leverett theory to derive key water flood parameters. Table II shows the complete matrix of the relative permeability combination. Each forward run of the model involves a pair of oil and water relative permeability functions, shown in the table $K_{ro}^a K_{rw}^b$, where a and b refer to either the P_{10} (l), P_{90} (u), mean (m) or the maximum likelihood (ml) functions. The truth case is designated by (tr).

Figure 5(a) shows plots of the fractional flow of water, as a function of the water saturation. Notably, the uncertainty envelope defined by $K_{ro}^l K_{rw}^u$ and $K_{ro}^u K_{rw}^l$, fully encapsulates the fractional flow functions. Figure 5(b) shows the efficiency of the core flood procedure. It shows the volume of oil

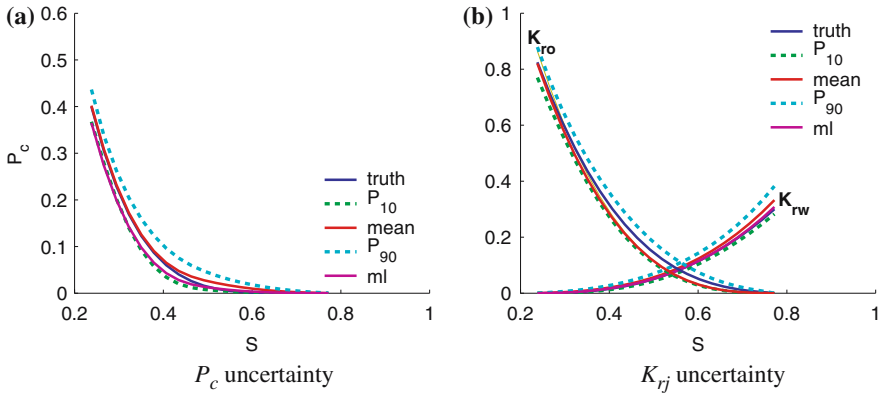


Figure 4. Uncertainty in flow functions.

Table II. Model matrix

$K_{ro}^l K_{rw}^l$	$K_{ro}^l K_{rw}^l$	$K_{ro}^l K_{rw}^m$	$K_{ro}^m K_{rw}^m$	$K_{ro}^l K_{rw}^u$	$K_{ro}^m K_{rw}^u$	$K_{ro}^u K_{rw}^u$
$K_{ro}^u K_{rw}^l$	$K_{ro}^{ml} K_{rw}^{ml}$	$K_{ro}^u K_{rw}^m$	$K_{ro}^{tr} K_{rw}^{tr}$			

produced as a function of the volume of water injected, quantified in terms of the pore volume (PV) of the porous medium. Figure 5(b) shows that the apparently narrow uncertainty in the relative permeability curves, leads to an uncertainty of about 10% pore volumes in the prediction of recoverable oil during water flooding. This, in real field terms, can lead to high uncertainty in any decisions, which depend on an estimate of the recovery efficiency, e.g., enhanced oil recovery strategies, economic and managerial decisions.

Figure 5(c) shows the water saturation profile as a function of the distance from the water injection end, before the water breakthrough. It also indicates the shock height for the truth, maximum likelihood (ml), $K_{ro}^l K_{rw}^u$ (upper bound) and $K_{ro}^u K_{rw}^l$ (lower bound). We note here that the bound defined by the lower and upper bounds rightly encapsulate the truth and maximum likelihood behavior. In terms of real field simulation, the information in Figure 5(a) and (c) give indications to the possible sweep efficiency of a planned water flood project.

Figure 5(d) gives explicit information about how much residual oil is to be expected during water flooding of the porous medium. For a given pore volume of injected water, one can determine the water saturation to be expected and therefore the corresponding residual oil saturation. This figure shows that there is a large degree of uncertainty in the expected residual oil saturation. In summary, the maximum likelihood model appears to be highly accurate in predicting the truth.

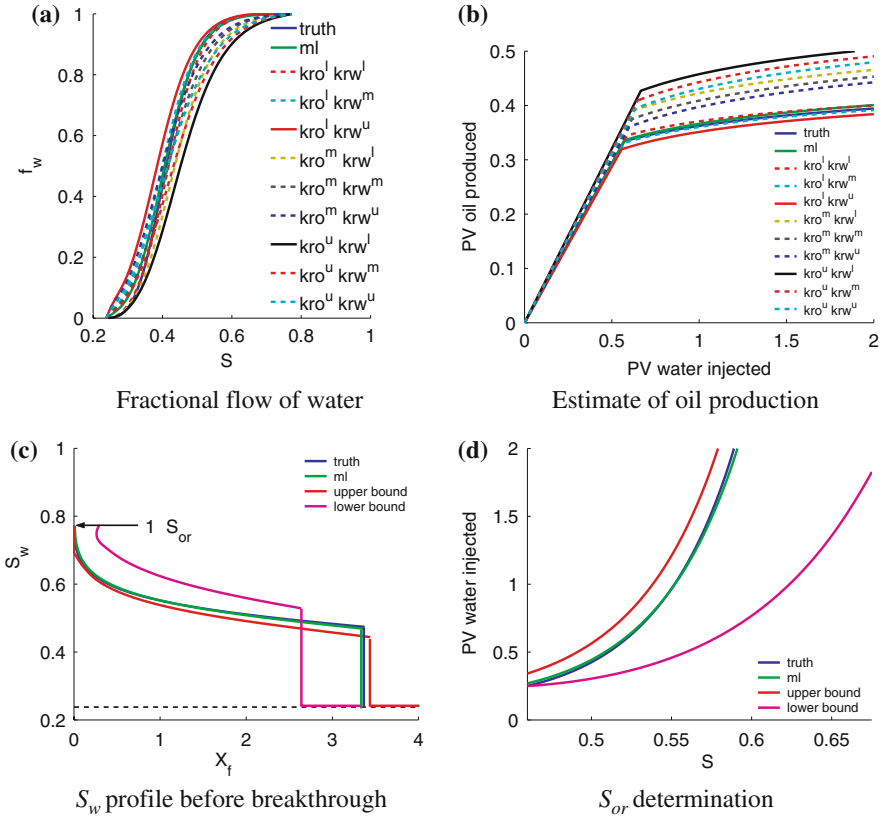


Figure 5. Uncertainty in homogeneous model.

The homogeneous case characterizes an ideal field situation representing relatively thin reservoir intervals, where diffuse or dispersed flow is assumed. This implies that over any part of the cross-section, the saturation of oil and water are uniform and no fluid segregation exists (Archer and Wall, 1991).

Since petroleum reservoirs are usually heterogeneous, of interest is how the uncertainty in the in-phase flow functions impact on, e.g., the hydrocarbon recovery uncertainty. Using the synthetic field model, we investigated the effect of core scale uncertainty on the full field recovery efficiency. Figure 6(a) shows the uncertainty in the oil recovery efficiency, while Figure 6(b) shows the relative error in the $P_{10} - P_{90}$ estimates, with respect to the truth. This plot shows that we can expect an error between 10% and 30%, in the estimate of recovery efficiency. This uncertainty could have serious impact on any decisions based on expected recovery and economic returns.

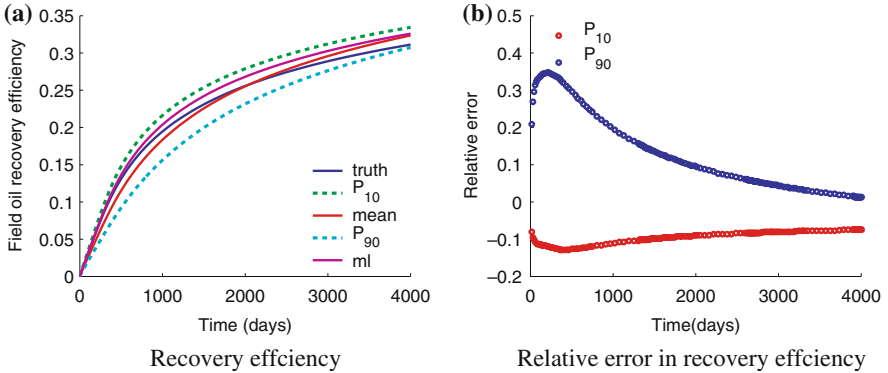


Figure 6. Uncertainty in recovery efficiency – heterogeneous model.

8. Summary and Conclusions

Using synthetic data, we have demonstrated a method for deriving relative permeability and capillary pressure functions from uncertain, unsteady-state laboratory data. Our approach involves generating multiple flow functions, which can reproduce the experimental data within some tolerance. We have used the NA algorithm in generating the family of solutions and shown how an error bound, which captures the truth, could be generated, by re-sampling from the posterior distribution.

Results presented in this paper show that the use of rigid analytical representation of the in-phase flow functions could introduce further uncertainty in the derived flow functions. The use of flexible functions, capable of capturing local effects, e.g., splines functions or Bernstein polynomials, is a viable alternative. Using normalized B-spline basis functions implies that for n model parameters the parameter space is confined to lie within an n -dimensional cuboid, thus eliminating the problem of rescaling the parameter space. In history matching models with high throughput, this approach of restricting the parameter space to regions, which contain physically acceptable solutions, is desirable.

We have investigated the impact of the uncertainty in the flow function on the oil recovery efficiency of two types of synthetic reservoir models. For this particular example, our results indicate that the core scale uncertainties have significant impact on the performance of both homogeneous and heterogeneous reservoirs.

Our results, however, are dependent on the definition of the performance index, which quantifies the misfit surface. In this, paper, we have made non-rigorous estimates of the data correlation and variance. A future paper will address this issue using a more rigorous approach.

Acknowledgements

The authors are grateful to the sponsors (Anadarko, BG, BP, ConocoPhillips, DTI, ENI, JNOC, Landmark, Shell and Statoil) of the Uncertainty and Upscaling research at Heriot-Watt University for funding. We are also grateful to Schlumberger-GeoQuest for the use of the Eclipse simulator.

References

- Akin, S., Castanier, L. M. and Brigham, W. E.: 1999, Effect of temperature on heavy oil/water relative permeabilities, *Soc. Petrol. Eng. J.* **54120**, 1–11.
- Archer, J. S. and Wall, P. G.: 1991, *Petroleum Engineering: Principles and Practice*, Graham & Trotman, London.
- Archer, J. S. and Wong, S. W.: 1973, Use of a reservoir simulator to interpret laboratory waterflood data, *Soc. Petrol. Eng. J.* **3551**, 343–347.
- Buckley, S. E. and Leverett, M. C.: 1942, Mechanisms of fluid displacement in sands, *Trans. Am. Inst. Min. Eng.* **146**, 107–116.
- Chavent, G., Cohen, G. and Espy, M.: 1980, Determination of relative permeabilities and capillary pressures by an automatic adjustment method, *Soc. Petrol. Eng.* **9237**, 1–10.
- Chierici, G. L.: 1981, Novel relations for drainage and imbibition relative permeabilities. *Soc. Petrol. Eng.* **10165**, 1–10.
- Christie, M. A.: 1996, Upscaling for reservoir simulation, *Soc. Petrol. Eng.* **37324**, 1–5.
- Christie, M. A. and Blunt, M. J.: 2001, Tenth SPE Comparative Solution Project: a comparison of upscaling techniques, *Soc. Petrol. Eng.* **66599**, 1–9.
- Civan, F. and Donaldson, E. C.: 1987, Relative permeability from unsteady-state displacements: an analytical interpretation, *Soc. Petrol. Eng.* **16200**, 139–155.
- Civan, F. and Donaldson, E. C.: 1989, Relative permeability from unsteady-state displacements with capillary pressure included, *SPE Form. Eval.* (June) 189–193.
- Collins, E. R.: 1976, *Flow of Fluids through Porous Materials*, PennWell Books, Tulsa, Oklahoma.
- Corey, A. T.: 1954, The Interrelation between gas and oil permeabilities, *Producers Monthly* **19**, 38–41.
- Craig, F. F. Jr.: 1971, *The Reservoir Engineering Aspects of Waterflooding*, Society of Petroleum Engineers of AIME, New York.
- Floris, F. J. T., Bush, M. D., Cuypers, M., Roggero, F. and Syversveen, A. R.: 1999, Comparison of production forecast uncertainty quantification methods – an integrated study, in: *Proceedings of 1st Conference on Petroleum Geostatistics*, Toulouse, France, pp. 1–20.
- Gabbanelli, S. C., Mezzatesta, A. G. and Bidner, M. S.: 1982, One-dimensional numerical simulation of waterflooding an oil reservoir. *Lat. Am. J. Heat Mass. Transf.* **6**, 251–273.
- Geman, S. and Geman, D.: 1984, Stochastic relaxation, Gibbs distributions and the Bayesian restoration of images, *IEEE Trans. Pattern Anal. Mach. Int.* **6**, 721–741.
- Gill, P. E. and Murray, W.: 1981, *Practical Optimization*, Academic Press, New York City.
- Glimm, J., Hou, S., Lee, Y. H., Sharp, D. and Ye, K.: 2001, Prediction of oil production with confidence intervals. *Soc. Petrol. Eng.* **66350**, 1–15.
- Glimm, J., Hou, S., Kim, H. and Sharp, D. H.: 2001, A probability model for errors in the numerical solutions of a partial differential equation, *Fluid Dyn. J.* **9**, 485–493.
- Grattoni, C. A. and Bidner, M. S.: 1990, History matching of unsteady-state corefloods for determining capillary pressure and relative permeabilities, *Soc. Petrol. Eng.* **21135**, 1–8.

- Hansen, K. M., Cunningham, G. S. and McKee, R. J.: 1977, Uncertainty assessment for reconstruction based on deformable geometry, *Int. J. Imag. Syst. Technol.* **8**, 506–512.
- Honarpour, M., Koederitz, L. and Harvey, A. H.: 1986, *Relative Permeability of Petroleum Reservoirs*, CRC Press, Inc., Boca Raton, Florida.
- Johnson, E. F., Bossler, D. P. and Naumann, V. O.: 1959, Calculation of relative permeability from displacement experiments, *Trans. Am. Inst. Min. Eng.* **216**, 370–372.
- Kerig, P. D. and Watson, A. T.: 1987, A new algorithm for estimating relative permeabilities from displacement experiments, *Soc. Petrol. Eng. Reserv. Eval.* **2**(1), 103–112.
- MacMillan, D. J.: 1987, Automatic history matching of laboratory corefloods to obtain relative-permeability curves, *Soc. Petrol. Eng. Reserv. Eval.* **2**(1), 85–91.
- Marle, C. M.: 1981, *Multiphase Flow in Porous Media*, Gulf Pub. Co., Texas.
- Osoba, J. S., Richardson, J. G., Kerver, J. K., Hafford, J. A. and Blair, P. M.: 1951, Laboratory measurements of relative permeability, *Trans. Am. Inst. Min. Eng.* **192**, 47–56.
- Richardson, J. G., Kerver, J. K., Hafford, J. A. and Osoba, J. S.: 1952, Laboratory determination of relative permeability, *Trans. Am. Inst. Min. Eng.* **195**, 187–196.
- Richmond, P. C. and Watson, A. T.: 1990, Estimation of multiphase flow functions from displacement experiments, *Soc. Reserv. Eng.* **18569**, 1–7.
- Sambridge, M.: 1998, Exploring multidimensional landscapes without a map, *Inverse Probl.* **14**, 427–440.
- Sambridge, M.: 1999, Geophysical inversion with a neighbourhood algorithm – I. Searching a parameter space, *Geophys. J. Int.* **138** 479–494.
- Sambridge, M.: 1999, Geophysical inversion with a neighbourhood algorithm – II. Appraising the ensemble, *Geophys. J. Int.* **138**, 727–745.
- Savioli, G. B. and Bidner, M. S.: 1982, The influence of capillary pressure when determining relative permeability from unsteady-state corefloods, *Soc. Petrol. Eng.* **23698**, 1–10.
- Schumaker, L. L.: 1981, *Spline Functions: Basic Theory*, John Wiley & Sons, New York.
- Sigmund, P. M. and McCaffery, F. G.: 1979, An improved unsteady-state procedure for determining the relative-permeability characteristics of heterogeneous porous media, *Soc. Petrol. Eng. J.* **6720**, 1–14.
- Sivia, D. S.: 1996, *Data Analysis – A Bayesian Tutorial*. Clarendon Press, Oxford.
- Subbey, S.: 2000, Regularizing the Volterra Integral Equation – the Capillary Pressure Case. PhD thesis, University of Bergen, Norway.
- Subbey, S., Christie, M. and Sambridge, M.: 2002a, A strategy for rapid quantification of uncertainty in reservoir performance prediction, *Soc. Petrol. Eng.* **79678**, 1–12.
- Subbey, S., Christie, M. and Sambridge, M.: 2002b, Uncertainty reduction in reservoir modeling, *SIAM Contemp. Math.* **295**, 457–467.
- Subbey, S., Christie, M. and Sambridge, M.: 2004, The impact of uncertain centrifuge capillary pressure on reservoir simulation, *SIAM J. Sci. Comput.* **26**(2), 537–557.
- Tao, T. M. and Watson, A. T.: 1984, Accuracy of JBN estimates of relative permeability: part 1 – error analysis. *SPEJ* (April) 209–214.
- Tao, T. M. and Watson, A. T.: (1984), Accuracy of JBN estimates of relative permeability: part 2 – algorithms. *SPEJ* (April) 215–223.
- Tarantola, A.: 1987, *Inverse Problem Theory, Methods for Data Fitting and Model Parameter Estimation*, Elsevier Science Publishers, Amsterdam, The Netherlands.
- Watson, A. T., Kulkarni, R., Nordtvedt, J.-E., Sylte, A. and Urkedal, H.: 1998, Estimation of porous media flow functions, *Meas. Sci. Technol.* **9**, 898–905.
- Welge, H. J.: 1952, A simplified method for computing oil recovery by gas or water drive, *Trans. Am. Inst. Min. Eng.* **195**, 91–98.
- Willhite, G. P.: 1986, *Waterflooding*, Society of Petroleum Engineers, Richardson, TX.